UNIVERSIDAD NACIONAL AUTÓNOMA DE MÉXICO

POSGRADO EN CIENCIAS MATEMÁTICAS

FACULTAD DE CIENCIAS

UN ENFOQUE GEOMÉTRICO DE CONJUNTOS INVARIANTES DE SISTEMAS DINÁMICOS

QUE PARA OBTENER EL GRADO ACADÉMICO DE

MAESTRO EN CIENCIAS

P R E S E N T A

DAVID MEDINA HERNÁNDEZ

DIRECTOR DE LA TESINA: DR. PABLO PADILLA LONGORIA

MÉXICO, D.F. SEPTIEMBRE, 2008

A geometric approach to invariant sets of dynamical systems

David Medina
IIMAS, Universidad Nacional Autónoma de México
Cd. Universitaria 04510
México D. F.
México

Abstract

In this paper, it is presented a geometric framework to study invariant sets of dynamical systems associated with differential equations in $\mathbb{R}^2$. This framework is based on extremizing properties of invariant sets for an area functional. By applying of the steepest descent method to this functional it is obtained its numerical approximation in the cases of heteroclinic orbits and limit cycles.

1 Introduction

In this work [1] consider the area generated by a curve under the action of the flow defined by an autonomous differential equation in $\mathbb{R}^2$.

This approach has been considered by Smith [2] as well as by Li and Muldowney [3, 4, 5, 6, 7]. The first author establishes bounds on the Hausdorff dimension of ω-limit sets. The last two authors extend the Bendixson's criterion for nonexistence of periodic solutions and give stability results for some periodic orbits based on area functionals.

The main goal of this paper is compute invariant sets considering a functional

[1] jointly developed with Pablo Padilla and Ramón Plaza.

that describes the area that generates a curve under a flow and observing that the functional vanishes in invariant curves and its minimization properties show that its infimum is attained in some curve that lies in the class of continuous curves of any fixed length (see Theorem 1). This variational principle is used in order to obtain a numerical implementation that will give us an approximation to this curve by employing the steepest descent method, that which is a method to find a maximum (or minimum) of a function based in the fact that a function increases most quickly in the direction of its gradient.

This implementation is done in the cases of heteroclinic orbits and limit cycles.

2 The area functional and invariant sets

Given a dynamical system defined on a set X, its evolution is described by a monoparametric family of operators $\{S(t)\}_{t\geq 0}$, that maps X into itself and possesses the standard semigroup properties:

$$S(t+s) = S(t)\cdot S(s), \forall s,t \geq 0$$

and

$$S(0) = I.$$

The basic property about this family is: $S(t)$ is a continuous operator (in general nonlinear) from X into X.

A set $Y \subset X$ is *positively invariant* for $S(t)$ if

$$S(t)Y \subset Y, \forall t > 0 \tag{1}$$

or *negatively invariant* if

$$S(t)Y \supset Y, \forall t > 0. \tag{2}$$

When the set is both, positively and negatively invariant we say that it is an invariant set.

Thus, a set $Y \subset X$ is an invariant set for the semigroup $\{S(t)\}_{t\geq 0}$ if

$$S(t)Y = Y, \forall t \geq 0. \tag{3}$$

As the simplest examples of invariant sets are, the equilibrium points, heteroclinic orbits and limit cycles.

A *heteroclinic orbit* is a path in phase space that joins two different equilibrium points. One of them it is ω-limit set of this orbit and the other it is α-limit set.

A *limit cycle* is a closed trajectory in phase space such that any spiral trajectory approaches to it when t(or $-t$) increases.

In order to describe the characterization of invariant sets through an area functional, let us consider the case where $S(t)$ is generated by the differential equation

$$\dot{x} = f(x), \tag{4}$$

where f is a vector field in $\mathbb{R}^2$.

Thus, for a curve $\gamma(s)$, where γ is assumed to be parameterized by arc length $\gamma : [s_0, s_1] \to \mathbb{R}^2$, $S(t)\gamma(s)$, for some fixed $t \in [0, T]$ represents the *displaced curve* under the flow generated by S at time t. Analogously, if we consider $S(t)\gamma(s)$ for all $t \in [0, T]$ and all $s \in [s_0, s_1]$ we obtain a strip on the phase plane, as shown in figure 1. Approximation, up to first order in t, of the area generated by this curve under the flow assuming that x_0 and x_1 are fixed points of (4)
(i.e. $f(x_0) = 0$, $f(x_1) = 0$) and $\gamma(s)$ is a continuous curve that joins this points, with $\gamma(s_0) = x_0$ and $\gamma(s_1) = x_1$. Let Γ be the set of this curves.

Thus, the differential element of area, is given by $|f(\gamma(s)) \times \dot{\gamma}(s)|$, as shown in figure 2.

Therefore the area, $A_t(\gamma(s))$, up to first order in time, t, is given by:

$$A_t(\gamma(s)) = \left(\int_{s_0}^{s_1} |f(\gamma(s)) \times \dot{\gamma}(s)| \, ds \right) t + o(t^2). \tag{5}$$

It is clear that if the curve is invariant then $A_t(\gamma(s)) = 0$. The converse is also true under appropriate assumptions.

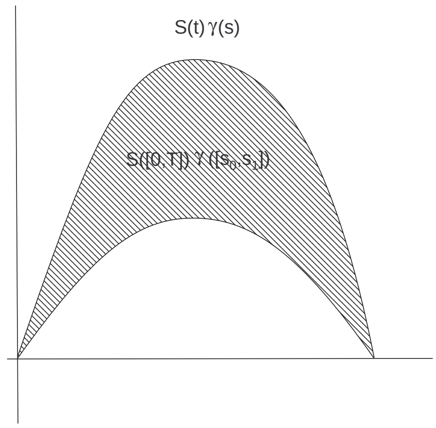

Figure 1: Strip generate by a curve under a flow.

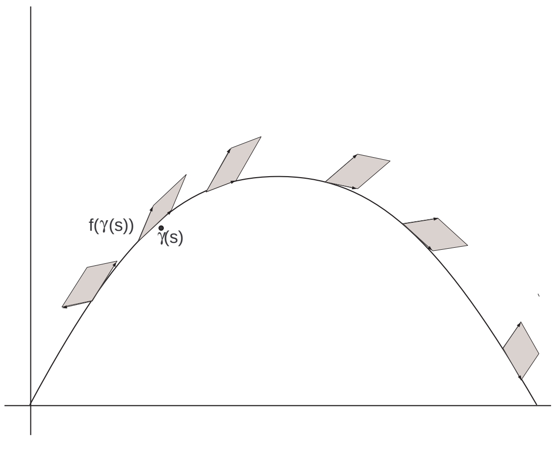

Figure 2: Differential element for the area functional.

Since the functional is bounded from below (clearly $A_t \geq 0$), then the natural way to study invariant sets is through the minimization of A_t.

Let be $A^*(\gamma) = \int_{s_0}^{s_1} |\dot{\gamma} \times f| \, ds$, l fixed and $\Gamma_l = \{\gamma \in \Gamma | \text{length}(\gamma) \leq l\}$. If the infimum of the area functional is zero in Γ and equal to infimum in Γ_l

then this infimum will be a invariant curve, as established in the following theorem.

Theorem 1. *If there is* 1 *such that* $\inf_\Gamma A = \inf_{\Gamma_l} A^*$ *and* $\inf_\Gamma A^* = 0$, *then* $\inf_\Gamma A^*$ *is attained in some* γ^* *that is invariant, under the flow generated by (4).*

Remark 1. In general, the equality $\inf_\Gamma A = \inf_{\Gamma_l} A^*$ does not hold, since $\Gamma_l \subset \Gamma$. This fact only implies that $\inf_\Gamma A \leq \inf_{\Gamma_l} A^*$.

Remark 2. Consider the phase portrait and in particular the orbits shown in figure 3. In this case, any curve that joins x_0 and x_1 with finite length generates area. The infimum does not attained in the class of curves with finite length, and therefore can not be a invariant curve.

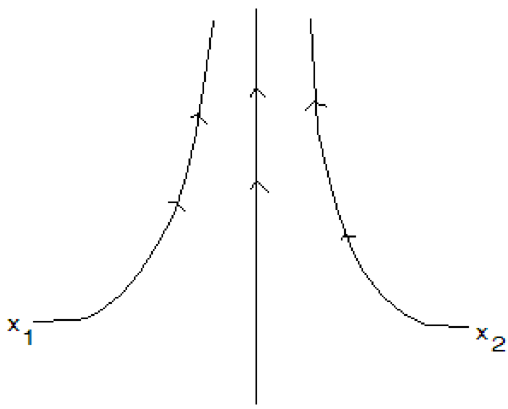

Figure 3: Phase portrait of some orbit with that is not an invariant curve.

Proof. Without loss of generality, can work in Γ_l. (Γ_l is bounded and equicontinuous by hypothesis).

Let γ_n be a minimizing sequence in Γ_l. By Arzela - Ascoli's theorem there is a subsequence γ_{n_j} such that $\gamma_{n_j} \stackrel{unif}{\longrightarrow} \gamma^*$.

By Fatou's lemma

$$0 \leq \int_{s_0}^{s_1} |\dot{\gamma}^* \times f(\gamma^*)| = \int_{s_0}^{s_1} \liminf |\dot{\gamma}_{n_j} \times f(\gamma_{n_j})| \leq \lim \int_{s_0}^{s_1} |\dot{\gamma}_{n_j} \times f(\gamma_{n_j})| \to 0.$$

Therefore $|\dot{\gamma}^* \times f(\gamma^*)| = 0$, $\forall$ s $\in [s_0, s_1]$. This implies that $\dot{\gamma}^*$ is parallel to $f(\gamma^*)$ and so γ^* is invariant for the flow generated by (4). $\square$

3 Numerical implementation

Theorem 1 guarantees that the infimum of the area functional is attained at some curve. However, we do not have an analytic or approximate expression. In what follows, shows that the variational principle can be used numerically to approximate this curve.

In order to obtain this approximation, employ the functional

$$\tilde{A}(\gamma(s)) = \int_{s_0}^{s_1} |f(\gamma(s)) \times \dot{\gamma}(s)|^2 \, ds, \tag{6}$$

because it is convenient from the numerical point of view.

Consider the physical pendulum and it is studied the separatrix curve, i. e., the two heteroclinic orbits that joins $(-\pi, 0)$ with $(\pi, 0)$ including these points, in the phase portrait.

The equation reads

$$\ddot{x} = -\sin x \tag{7}$$

or equivalently,

$$(\dot{x}, \dot{y}) = (y, -\sin x). \tag{8}$$

(7) and (8) constitute a conservative system (see [1]), in which the total energy E given by

$$E = \frac{1}{2}\dot{x}^2 + U(x)$$

where

$$U(x) = \int_0^x \sin\eta \, d\eta = 1 - \cos x,$$

is conserved. Its phase portrait is shown in figure 4.

The separatrix, lies on the level curve $E = 2$ and is given by

$$\frac{1}{2}y^2 - \cos x - 1 = 0. \tag{9}$$

Therefore the upper part of (9) is parameterized by

$$(s, \sqrt{2\cos s + 2}), \; -\pi \leq s \leq \pi. \tag{10}$$

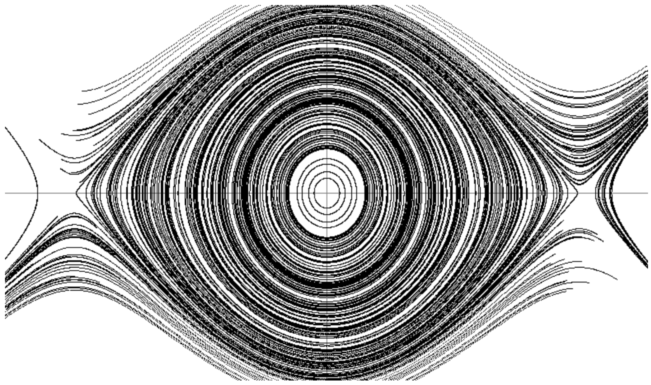

Figure 4: Phase portrait of the system (8).

Now, suppose that $(s, v(s))$ is an approximation to (10), which satisfies $v(\pm\pi) = 0$. Under this assumption, calculate the area functional $\tilde{A}$ given by (6) generated by the flow (8).

A straightforward calculation gives that $\tilde{A}(\gamma(s))$ for $\gamma(s) = (s, v(s))$ is

$$\tilde{A}(\gamma(s)) = \int_{-\pi}^{\pi} (\sin s + v(s)v'(s))^2 ds. \tag{11}$$

Now, we take

$$v(s) = -(s+\pi)(s-\pi)\sum_{i=0}^{n} a_i s^i, \tag{12}$$

which clearly satisfies $v(\pm\pi) = 0$.

Note that in (11), the a_i's values mentioned in (12) are taken as *variables*. For some choice of these values, we obtain a parameterized curve. Thus, we want to find the choice of these coefficients such that (12) be the *best approximation* to the invariant curve.

We need a method in order to obtain them. The steepest descent method (or gradient method) is one of the simplest and the most useful minimization methods for unconstrained optimization, which is based in successive approximations and consider the gradient of the function, because (its negative) represents the direction in which the function decreases most quickly.

The iteration reads:

$$x_{i+1} = x_i - \epsilon \nabla \tilde{A}(x_i), \tag{13}$$

where x_i is the i-th iteration , ϵ is a small value (we choose it) and $\nabla \tilde{A}(x_i)$ represents the gradient of area functional evaluated in the i-th iteration.

In order to determine the convergence of (13), we use the following criterion:

1. Select an parameter of tolerance $\delta > 0$.
2. Calculate $\mathbf{c} = \nabla f(x_i)$. If $\|\mathbf{c}\| < \delta$ then x_i it is the sought value, else repeat until obtain the parameter of tolerance chosen.

For a more detailed description about this method, see for example [8, 9].

Now, we choose $n = 2$ in (12), due to the symmetry of the separatrix with respect to y-axis, and consider the *initial guess* $(2.03, 0, -0.27)$ [2] and $\epsilon = 0.000009$.

The following code written in Maple© gives the coefficients in (12) such that $(s, v(s))$ is the approximation to (10).

```
> restart;
> v:=-a[0]*s^2-sum(a[k]*s^(k+2),k=1..2)+evalf(Pi^2)*a[0]+
  sum(evalf(Pi^2)*a[k]*s^k,k=1..2):
> vprime:=diff(v,s):
> u1:=apply(sin, s):
> u2:=(u1+v*vprime)*(u1+v*vprime):
> area:=Int(u2,s=-Pi..Pi):
  gradiente:=[seq(diff(area,a[k]),k=0..2)]:
  iteracion[0]:=[2.03,0,-.27]:
  for r from 0 to 2000 do:
  B:=seq(a[l]=iteracion[r][l+1],l=0..2):
  C:=subs(B,gradiente):
  gradienteevaluado[r]:=[seq(evalf(C[p]),p=1..3)];
  iteracion[r+1]:=[seq(iteracion[r][j]-0.000009*
  gradienteevaluado[r][j],j=1..3)];
  end do:
```

[2] Those values were chosen because represent and approximation to exact values in Taylor expand of (10)

The following code is used in order to obtain a graphical representation of both the curve obtained by this method and the curve obtained with an *initial guess*. This results are shown in figures 5 to 10.

```
> plot([[x,-sum(iteracion[50][z+1]*x^(z+2),z=0..2)+
  sum(evalf(Pi^2)*iteracion[50][z+1]*x^z,z=0..2),x=-Pi..Pi],
  [x,sqrt(2*cos(x)+2),x=-Pi..Pi]],color=[red,blue]);
```

In the application of the above criterion to this example, we choose $\delta = 0.0011$ and the corresponding value of the norm in the 2000-th iteration is 0.001055164525. This fact shows convergence of this method according to the criterion previously established.

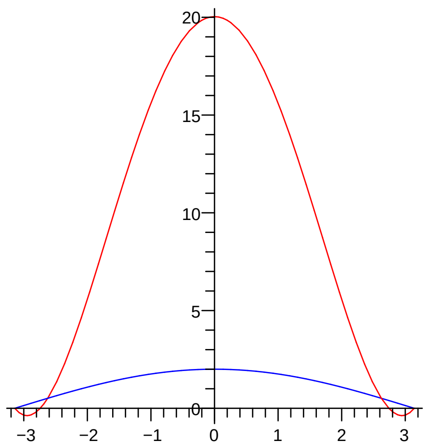

Figure 5: Initial curve versus invariant curve.

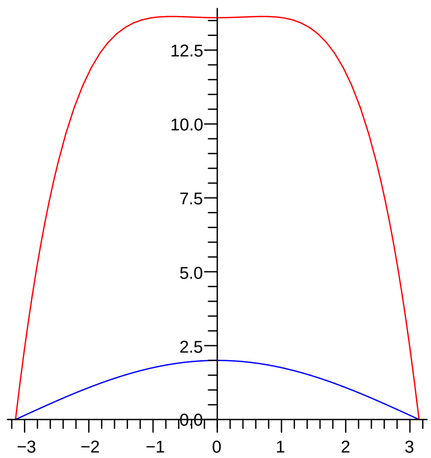

Figure 6: First iteration versus invariant curve.

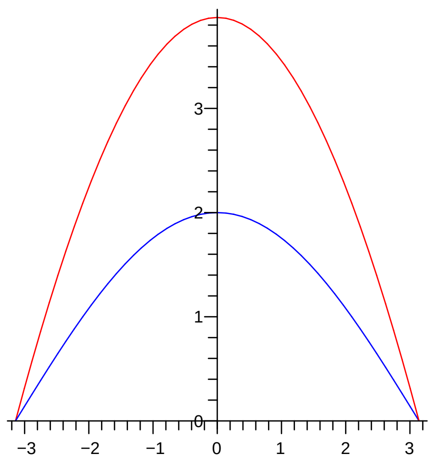

Figure 7: 50-th iteration versus invariant curve.

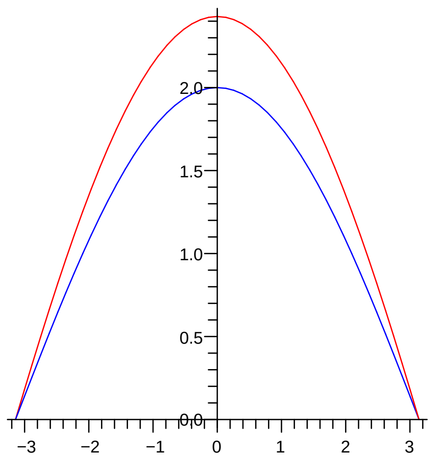

Figure 8: 100-th iteration versus invariant curve.

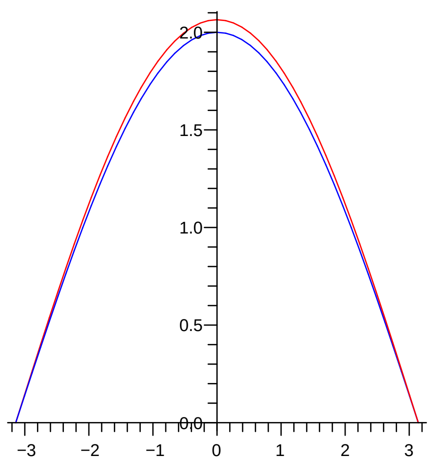

Figure 9: 500-th iteration versus invariant curve.

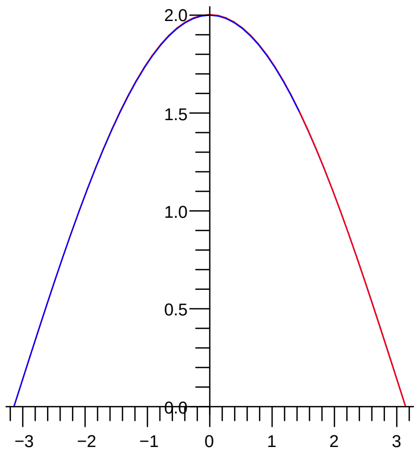

Figure 10: 1000-th iteration versus invariant curve.

On other hand, if we consider (clearly it is not satisfies $v(\pm\pi) = 0$)

$$v(s) = \sum_{k=0}^{n} a_k s^k \tag{14}$$

instead of (12), we choose $n = 11$ (a *truncated Taylor series*) and the initial guess:

$$(2.03, 0, -0.27, 0, 6 \times 10^{-3}, 0, -5 \times 10^{-5}, 0, 1.95 \times 10^{-7}, 0, -6 \times 10^{-10}) \tag{15}$$

We fix $\epsilon = 3 \times 10^{-10}$. A graphical representation of the initial curve is shown in figure 11. Then we obtain the curve after 10 iterations and compare it with the corresponding invariant curve (see figure 12).

If we consider another initial guess, which is slightly further apart from the invariant curve, in which the coefficients (components of initial guess) are the following:

$$(2.01, 0, -0.3, 0, 6 \times 10^{-3}, 0, -5 \times 10^{-5}, 0, 1.95 \times 10^{-7}, 0, -6 \times 10^{-10}) \tag{16}$$

The corresponding graphs after 10 iterations and the initial curve are shown in the figures 13 and 14, we keep the ϵ value as before.

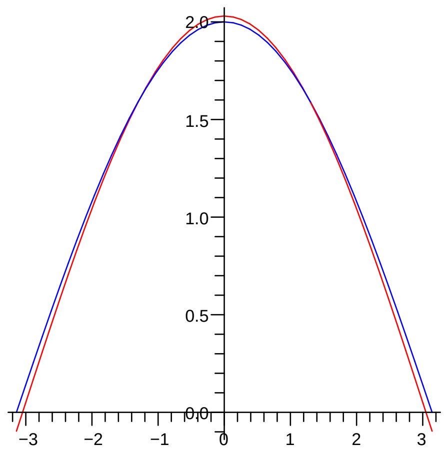

Figure 11: Initial curve versus invariant curve.

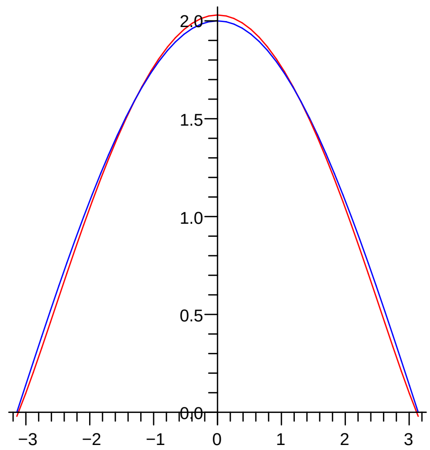

Figure 12: Graph of 10-th iteration versus invariant curve.

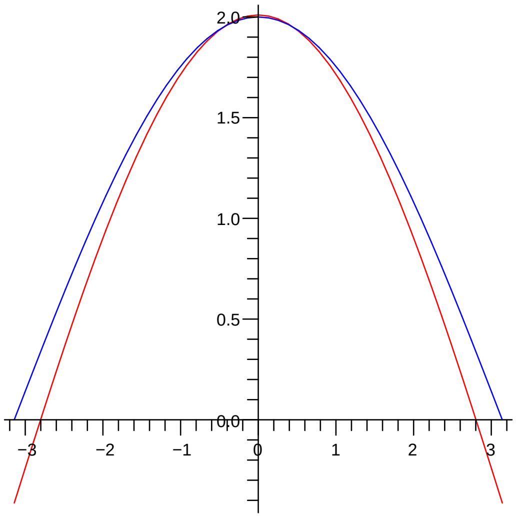

Figure 13: Initial curve versus invariant curve.

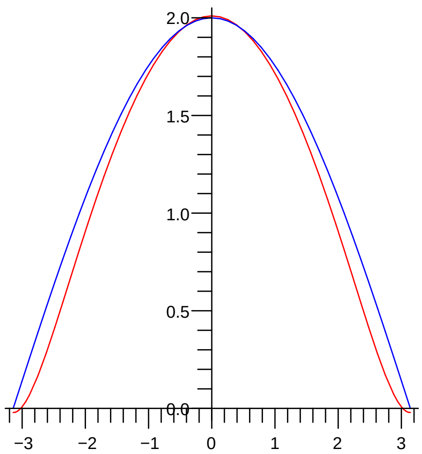

Figure 14: 10-th iteration versus invariant curve.

We also obtained another results for a small modification of the values of (16), in which we only take 2.1 in its first component instead of 2.01. The corresponding iterations are shown in figures 15 and 16.

As expected, when considering (14) - (16), the value of gradient of the area

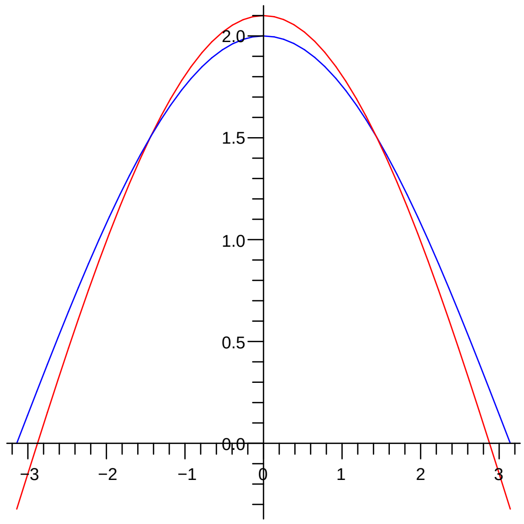

Figure 15: Initial curve versus invariant curve.

functional after 10 iterations is 2356.113011. Moreover, in subsequent iterations the convergence criterion does not hold, because the norm of gradient is big. Similar results are obtained in other cases. This fact shows that it is not a convenient choose.

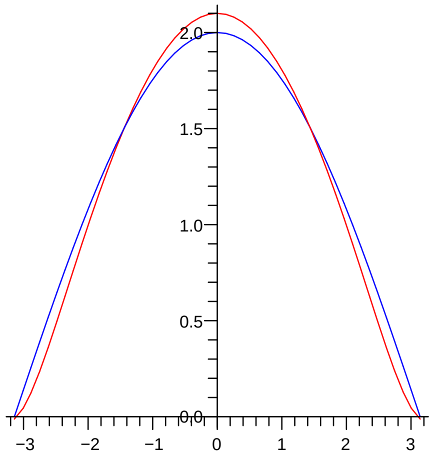

Figure 16: 10-th iteration curve versus invariant curve.

4 Application to limit cycles

In this section we shall see how to extend the above idea in the study of another invariant sets. The cases in consideration are limit cycles.

Since this sets are closed curves, we use truncated Fourier series instead of polynomials in order to approximate to them.

$$\dot{x_1} = -x_2 + x_1(x_1^2 + x_2^2 - 1) \quad (17)$$
$$\dot{x_2} = x_1 + x_2(x_1^2 + x_2^2 - 1) \quad (18)$$

By transformation to polar coordinates, we see that $x_1^2 + x_2^2 = 1$ is a stable limit cycle (see figure 17).

In order to characterize this limit cycle by minimization of functional $\tilde{A}$ given by (6), we use the usual parametrization

$$\gamma(s) = (\cos s, \sin s), \ 0 \le s \le 2\pi. \quad (19)$$

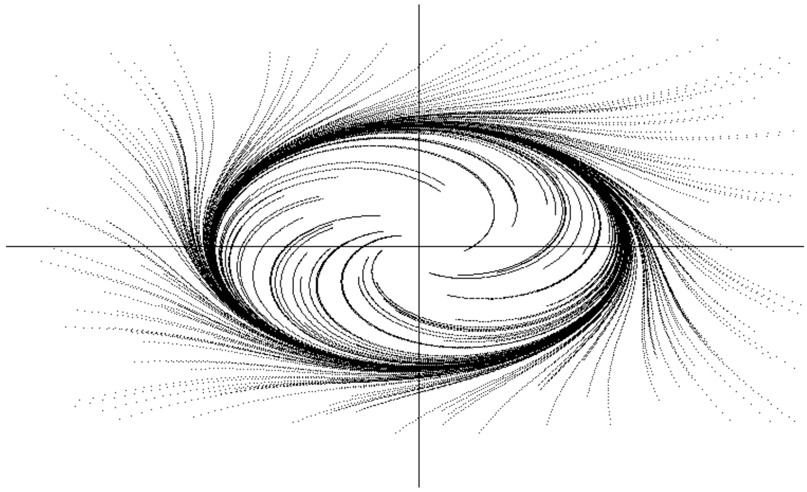

Figure 17: Phase portrait of (17) - (18).

Assume that

$$u(s) = \sum_{k=0}^{2} a_k \cos ks + \sum_{k=1}^{2} b_k \sin ks, \tag{20}$$

$$v(s) = \sum_{k=0}^{2} a'_k \cos ks + \sum_{k=1}^{2} b'_k \sin ks, \tag{21}$$

is a finite approximation to (19).

Therefore

$$\tilde{A}(\gamma(s)) = \int_0^{2\pi} ((-v + u(1-u^2-v^2))v' - (u + v(1-u^2-v^2))u')^2 \, ds \tag{22}$$

We choose $\epsilon = 0.005$ and $\delta = 0.0006$ in order to apply steepest descent method to this functional.

The corresponding initial guess is

$$(0, 1.3, 0.1, 0.1, 0.1, 0.1, 0.1, 0.01, 1.3, 0.1). \tag{23}$$

Since $|\nabla \tilde{A}(x_{110})| < 0.0006$, we obtain convergence as shown in figures 18 - 22.

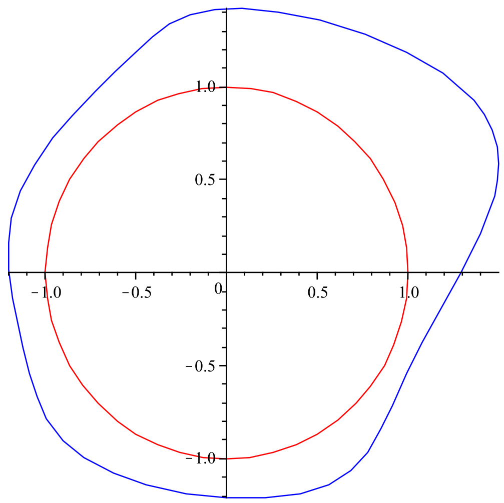

Figure 18: Initial guess versus stable limit cycle of (17)-(18).

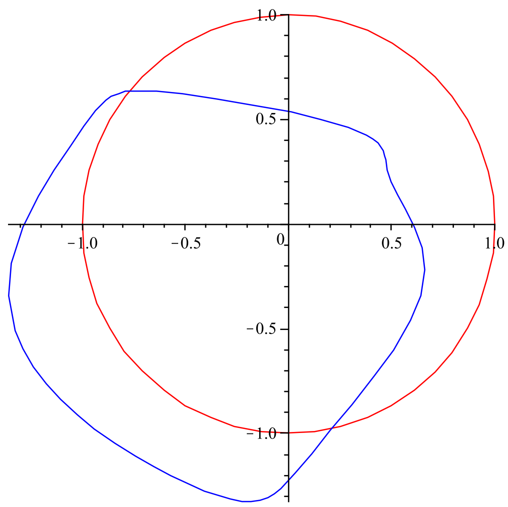

Figure 19: First iteration versus stable limit cycle.

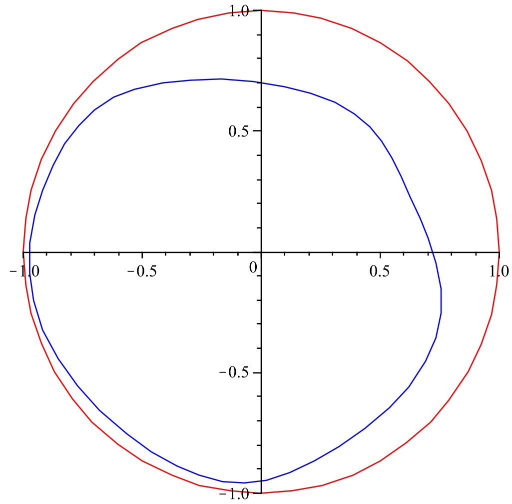

Figure 20: 10-th iteration versus stable limit cycle.

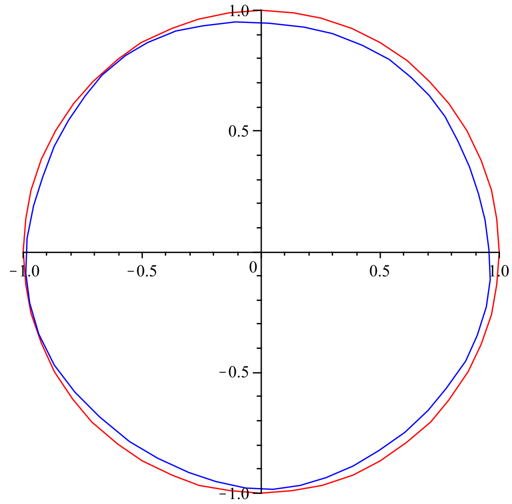

Figure 21: 50-th iteration versus stable limit cycle.

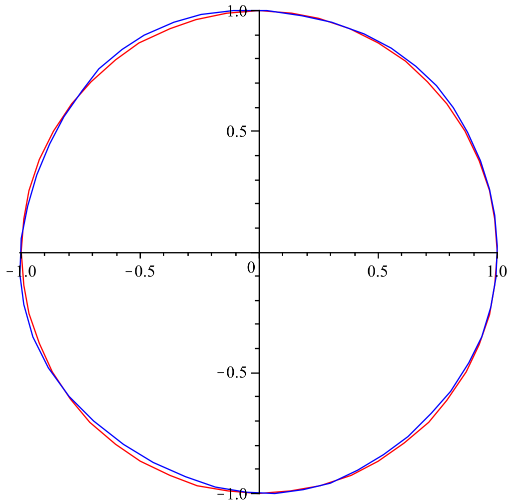

Figure 22: 111-th iteration versus stable limit cycle.

On other hand, if we consider

$$\dot{x_1} = -x_2 + x_1(x_1^2 + x_2^2 - 1)^2 \tag{24}$$
$$\dot{x_2} = x_1 + x_2(x_1^2 + x_2^2 - 1)^2 \tag{25}$$

instead of (17) - (18), then $x_1^2 + x_2^2 = 1$ is an unstable limit cycle (see figure 23).

As before, we employ (20) - (21), $\epsilon = 0.005$, $\delta = 0.0055$ and the initial guess:

$$(0, 1.2, 0.1, 0.1, 0.1, 0.1, 0.1, 0.01, 1.1, 0.1). \tag{26}$$

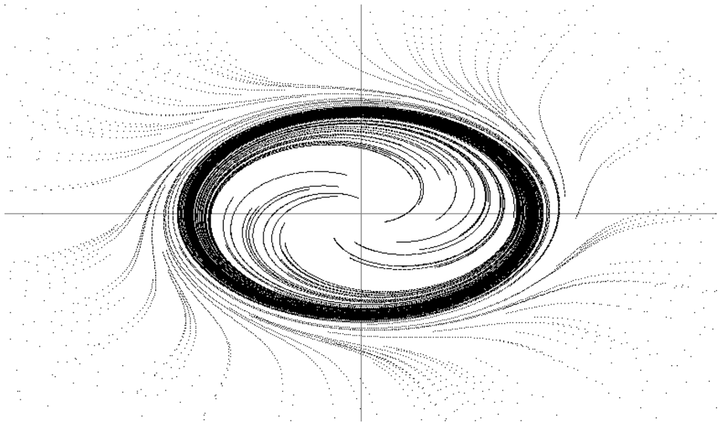

Figure 23: Phase portrait of (24) - (25).

Since $|\nabla \tilde{A}(x_{400})| < 0.0055$, we obtain convergence as shown in figures 24 to 28.

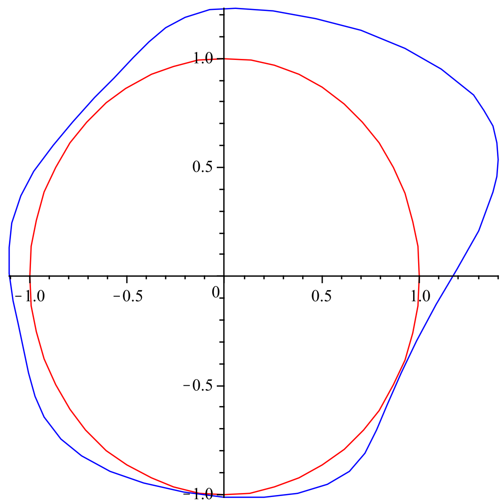

Figure 24: Initial guess versus stable limit cycle of (24)-(25).

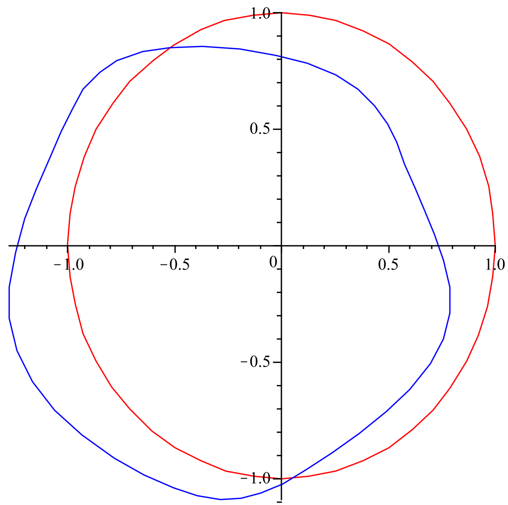

Figure 25: First iteration.

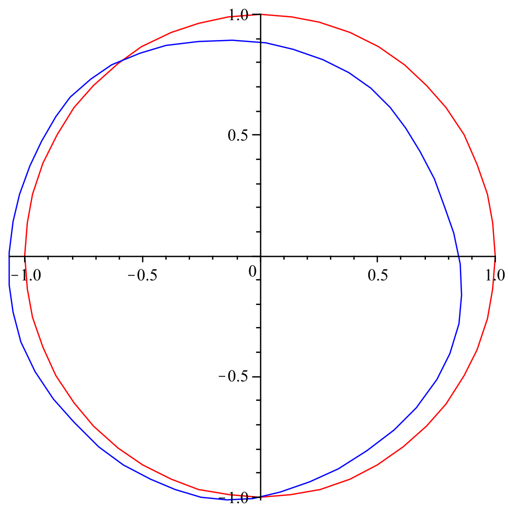

Figure 26: 10-th iteration versus stable limit cycle.

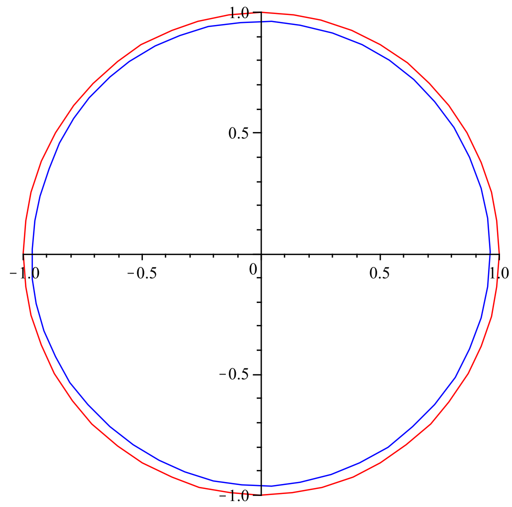

Figure 27: 100-th iteration versus unstable limit cycle.

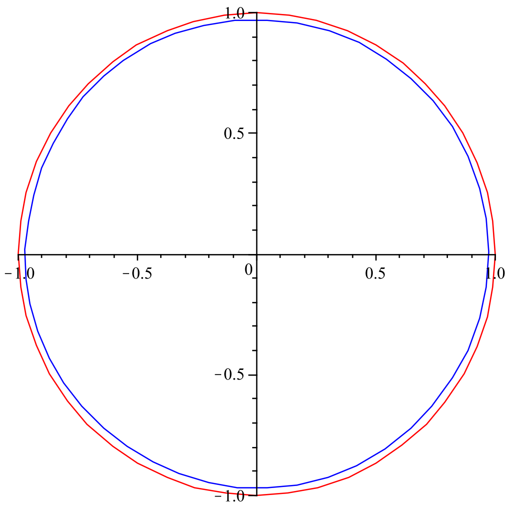

Figure 28: 110-th iteration versus unstable limit cycle.

References

[1] Arnold V. I.,*Mathematical Methods of Classical Mechanics*, Graduate Text in Mathematics, Springer - Verlag, 1989.

[2] Smith R. A.,*Some Applications of Hausdorff dimension inequalities for ordinary differential equations*, Proy. Roy. Soc. Edinburg Sect. A 104, 235 - 259, 1986.

[3] Li Yi M. and Muldowney James S., *On R. A. Smith's autonomus convergence theorem*, Rocky Mountain Journal of Mathematics, volume 25, number 1,365 - 381, 1995.

[4] Li Yi M. and Muldowney James S., *On Bendixson's Criterion*, Journal of Differential Equations 106, 27-39, 1993.

[5] Li Yi M. and Muldowney James S., *Evolution of surface functionals and differential equations*, Ordinary and Delay Differential Equations, Longman Scientific and Technical, 144 - 148, 1992.

[6] Li Yi M. and Muldowney James S., *Lower bounds for the Haussdorff dimension of attractors*, Journal of Dynamics and Differential Equations 7, 455 - 467, 1995.

[7] Li Yi M. and Muldowney James S., *Dynamics of differential equations on invariant manifolds*, Journal of Differential Equations 168, 295 - 320, 2000.

[8] Bonnans J. F., et. al. *Numerical Optimization: Theoretical and Practical Aspects*, Universitext, Springer-Verlag, 2006.

[9] Peressini A. L., et. al., *The Mathematics of Nonlinear Programming*, Undergraduate Text in Mathematics, Springer-Verlag, 1988.